AIP | Applied Physics Letters

A stable high-speed rotational transmission system based on nanotubes

Kun Cai, Hang Yin, Ning Wei, Zhen Chen, and Jiao Shi

Citation: Applied Physics Letters **106**, 021909 (2015); doi: 10.1063/1.4905696
View online: http://dx.doi.org/10.1063/1.4905696
View Table of Contents: http://scitation.aip.org/content/aip/journal/apl/106/2?ver=pdfcov
Published by the AIP Publishing

A stable high-speed rotational transmission system based on nanotubes

Kun Cai,[1,2,a)] Hang Yin,[1] Ning Wei,[1] Zhen Chen,[2,3] and Jiao Shi[3]
[1]*College of Water Resources and Architectural Engineering, Northwest A&F University, Yangling 712100, China*
[2]*State Key Laboratory of Structural Analysis for Industrial Equipment, Department of Engineering Mechanics, Faculty of Vehicle Engineering and Mechanics, Dalian University of Technology, Dalian 116024, China*
[3]*Department of Civil & Environmental Engineering, University of Missouri, Columbia, Missouri 65211-2200, USA*

(Received 26 November 2014; accepted 28 December 2014; published online 14 January 2015)

A stable rotational transmission system is designed with a single-walled carbon nanotube (SWCNT)-based motor and double-walled carbon nanotubes (DWCNTs)-based bearing. The system response is investigated using molecular dynamics (MD) simulation. It is found that the rotating motor can actuate the rotation of the inner tube in bearing because of the attraction between the two adjacent coaxial ends of motor and rotor (the inner tube in bearing). To have a stable nanostructure, each carbon atom on the adjacent ends of motor and rotor is bonded with a hydrogen atom. To obtain a stable high-speed rotational transmission system, both an armchair and a zigzag model are used in MD simulation. In each model, the motor with different diameters and rotational speeds is employed to examine the rotational transmission of corresponding DWCNTs. It is demonstrated that the long range van der Waals interaction between the adjacent ends of motor and rotor leads to a stable configuration of the adjacent ends, and further leads to a stable rotation of rotor when driven by a high-speed motor. As compared with the armchair model, the rotor in the zigzag model could reach a stable rotation mode much easier. © *2015 AIP Publishing LLC*.
[http://dx.doi.org/10.1063/1.4905696]

Ever since Cumings and Zettl[1] experimentally showed the ultralow friction force among the adjacent walls of multiwall carbon nanotubes (MWCNTs) by making the core tubes slide out of the MWCNTs, CNTs have been considered as potential nano-devices in the next generation of nano-electro-mechanical systems (NEMS). Due to the ultralow friction, a lot of nano-devices made from MWCNTs have been proposed over the last decade, such as gigahertz oscillators,[2,3] bearings,[4,5] nanopump,[6,7] and motors.[8–11] All these applications are based on the axial linear and/or rotational movements of CNTs. As compared with the rotational motion, the linear motion is relatively easy to achieve[1,12] and observe. For instance, Fennimore *et al.*[13] constructed a rotary motor with a metal plate motor attached to the outer shells of MWCNTs and activated by three stator electrodes. Soon after that, Bourlon *et al.*[14] changed the attachment position of the rotational plate to the rotors of MWCNTs. Although the rotational frequency of such a rotor designed with these methods is only a few hertz, it provided a feasible way to rotate MWCNTs axially, and resulted in many related applications. For example, Barreiro *et al.*[9] reported a cargo delivery system with both rotational and linear motion driven by a thermal gradient along a CNT. Using experimental and simulation methods, Somada *et al.*[10] observed the coupling motion of short-capped CNT into a CNT shell with the environmental temperature varying between 1073 and 1373 K. These types of motion can be regarded as CNT-based motors.[11] To drive the rotation of motor, Vacek and Michl[15] suggested three possible ways, namely, electric field, gas or liquid flow, and light absorption. For instance, Tu and Hu[16] presented a design of an electrical motor by applying the axially varying voltage under an isothermal condition. Wang *et al.*[17] established a simulation model for a rotary motor with one CNT shaft and three or six blades, which was excited by an external electric field. Kang and Hwang[18] simulated a high-speed rotational CNT motor activated by controlling the density and flow rate of fluidic gas. The rotational frequency of motor was ~240 GHz. Prokop *et al.*[19] proposed a molecular motor with gigahertz rotational frequency, using electric field and gas flow, respectively. In addition to the above methods, Xu *et al.*[20] studied the thermally driven behavior of double-walled carbon nanotubes (DWCNTs), and introduced a self-activated rotation of inner tube. Recently, we[21] revealed the mechanism of a rotary motor made from DWCNTs and driven by uniform environmental temperature. We found that the rotational frequency of the inner tube in a fixed outer tube could be over 160 GHz. In an NEMS, either linear or rotational motion of the inner tube in an outer tube is a signal/state of system. Hence, the rotational transmission can be considered as signal transmission. Up to now, however, no work has been reported on the design of rotational transmission system. In the present work, hence, a rotational transmission system is designed by using a single-walled carbon nanotube (SWCNT)-based motor and DWCNT-based bearing coaxially. To obtain a stable nanostructure, the atoms on the adjacent ends of rotating motor and rotor in bearing are bonded with hydrogen atoms.[22] Molecular dynamics (MD) simulations are performed to investigate the system response.

[a)]Author to whom correspondence should be addressed. Electronic mail: caikun1978@163.com

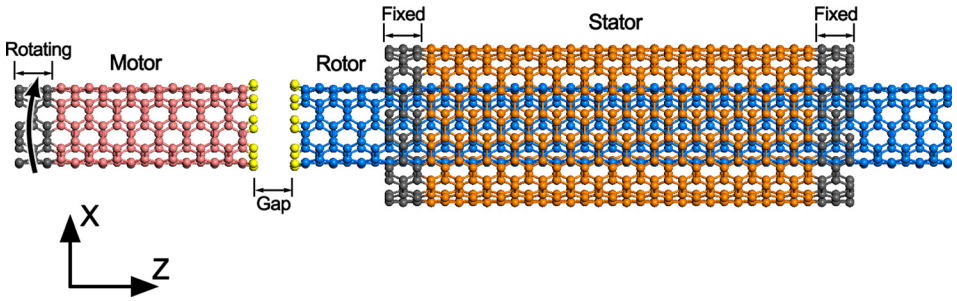

FIG. 1. Schematic of the proposed rotational transmission system consisting of a (5, 5) SWCNT-based motor and (5, 5)/(10, 10) DWCNTs-based bearing.

A rotational transmission system is designed as shown in Figure 1, which contains a motor made from a SWCNT and a bearing from DWCNT. The motor and bearing are coaxially arranged. The carbon atoms on the adjacent ends of motor and bearing are covalently combined with hydrogen atoms (yellow atoms). In our MD simulation, the adaptive intermolecular reactive empirical bond order (AIREBO) potential[23] is chosen to describe the effects of both the covalent bonds with carbon and hydrogen atoms and the long-range van der Waals interaction force. Two types of transmission system models, i.e., armchair and zigzag chirality models, are considered in simulation. Figure 1 demonstrates an armchair model, in which there is a (5, 5) SWCNT motor and (5, 5)/(10, 10) DWCNTs bearing. In the armchair model, two different motors, (5, 5) and (9, 9) motor, are considered to drive the same bearing. In the zigzag model, the bearing is (9, 0)/(18, 0) DWCNTs, and the chirality of motor is either (9, 0) or (16, 0).

Before simulation, a Nosé-Hoover heat bath at 300 K is applied for 100 ps relaxation of system. After relaxation, a constant rotational speed is specified on the motor. Meanwhile, the axial translational motion of motor and rotor is constrained. The whole system is under the canonical NVT ensemble with T = 300 K. The duration of each simulation is 5 ns with the time step of 1 fs.

In simulation, the rotor will be driven to rotate or oscillate along the axis because of the interaction between the adjacent ends of motor and rotor. Figure 2 illustrates the time histories of rotors' rotational frequency driven by different motors with different values of rotational frequency. In most cases as shown in Figure 2, the rotational frequency of rotors is lower than that of the motor, which indicates the existence of asynchronous transmission. In addition, most of the rotors exhibit unstable rotations. Even when the rotational frequency of motor is lower than 100 GHz, it is still difficult to activate a stable rotational motion of rotor. However, the (5, 5) motor with rotational frequency of 50 GHz or 100 GHz, the chirality of which is the same as that of rotor, could drive an approximately synchronous rotation of rotor (Figure 2(a)). Driven by the (5, 5) motor, a stable asynchronous rotation of rotor can occur when the rotational frequency of motor is very high, e.g., 200 or 250 GHz, and the average rotational frequency difference between the rotor and (5, 5) motor is about 100 GHz. The physics behind the above phenomena could be qualitatively explained here. The potential barriers[24] are along the axis in an armchair bearing and the axial linear motion is more stable than the rotation. Furthermore, the weaker attraction between rotor and motor with the lower rotational speed could result in a poor rotational transmission. It is known that the friction between the outer tube and inner tube in bearing depends on four factors, namely, the difference between the radii of stator and rotor, the overlap area,[25] the relative motion between two tubes and the environmental temperature.[14,21] The intertube friction within bearing is especially sensitive to the relative motion between tubes. Meanwhile, the interaction between the adjacent ends of motor and rotor relies on such factors as the distance (see Figure 5) and the relative rotational speed between motor and rotor, temperature, and the atom types on the ends. When the attraction between motor and rotor is weaker than the friction within bearing, it is difficult for the stable rotational transmission to happen.

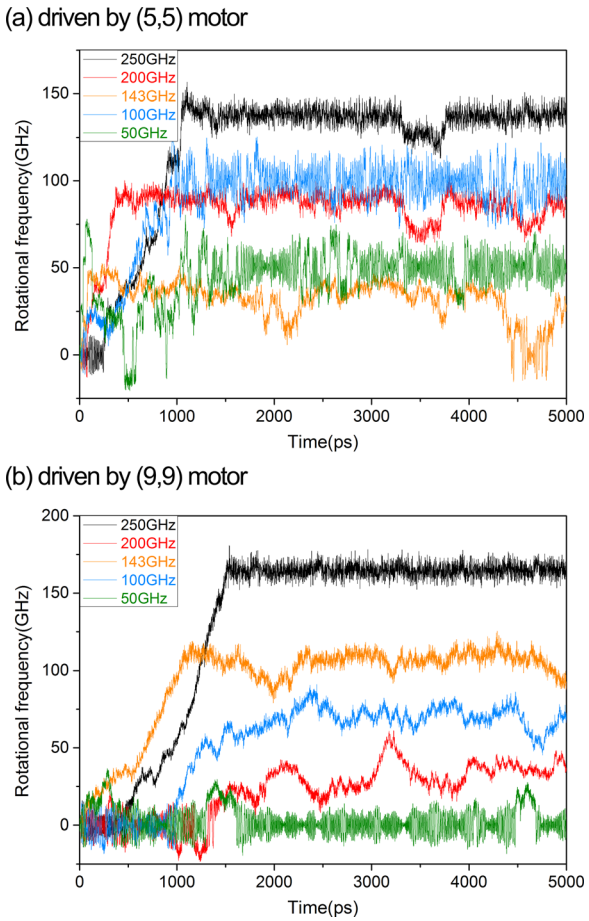

FIG. 2. For the armchair models, the time histories of rotational frequency of rotor driven, respectively, by (5, 5) and (9, 9) motors are shown with different values of motor's rotational frequency/period (black curve: 250 GHz/4 ps, red curve: 200 GHz/5 ps, orange curve: 143 GHz/7 ps, blue curve: 100 GHz/10 ps, and green curve: 50 GHz/20 ps).

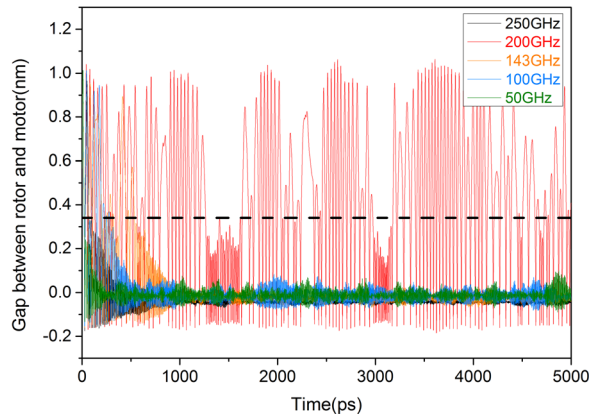

FIG. 3. The distance gap between rotor and motor when driven by the (9, 9) motor with different values of rotational frequency. Dashed line represents the initial gap (0.34 nm). The negative gap indicates that the rotor partly enters into the motor.

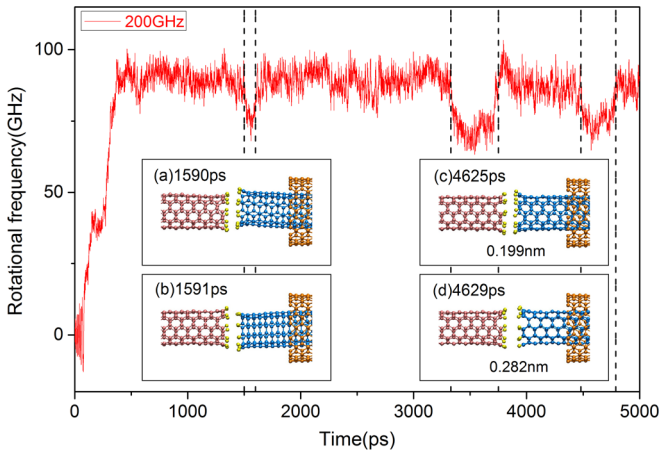

FIG. 4. Detailed demonstration of the behavior of the rotor driven by the (5, 5) motor with 200 GHz rotational frequency.

When driven by the (9, 9) motor (Figure 2(b)), the rotation behavior of rotor depends on the rotational frequency of motor more obviously than the (5, 5) motor. As can be seen, the most stable rotation of rotor is obtained after 1500 ps when the rotational frequency of motor is 250 GHz. A relatively stable rotation of rotor can also be obtained when the rotational frequency of motor is 143 GHz. However, the rotational behavior of rotor driven by the (9, 9) motor with rotational frequency of 200 GHz is poorer than that driven by the motor with 100 GHz. Observing the oscillation of the rotor driven by the (9, 9) motor with 200 GHz, one can find that the average rotational frequency of rotor is lower than 50 GHz and that the oscillation of rotor has a nearly stable period and amplitude (see Figure 3). Hence, the inner tube acts as a pretty oscillator[3] rather than a rotor. Due to the perfect oscillation, the torque applied to the rotor by the motor with 200 GHz also fluctuates, and the resultant torque at the same simulation steps is far less than that by the motor with a lower rotational frequency (e.g., 100 GHz). Therefore, the rotational frequency of motor is lower than that driven by the motor with 100 GHz.

Figure 4 gives a detailed demonstration of the rotational behavior driven by the (5, 5) motor with 200 GHz rotational frequency. The activated rotation of rotor fluctuates with a big jump during 1500^{th}–1600^{th} ps, 3330^{th}–3750^{th} ps, and 4480^{th}–4790^{th} ps (indicated with dashed lines in Figure 4). The balanced distance between two hydrogen atoms is 0.265 nm in Lennard-Jones (L-J) (6–12) potential formulation. When the gap between the adjacent ends of motor and rotor is less than 0.265 nm, the repulsive interaction dominates between the hydrogen atoms on both ends. But the hydrogen atoms on motor are attracted by the carbon atoms

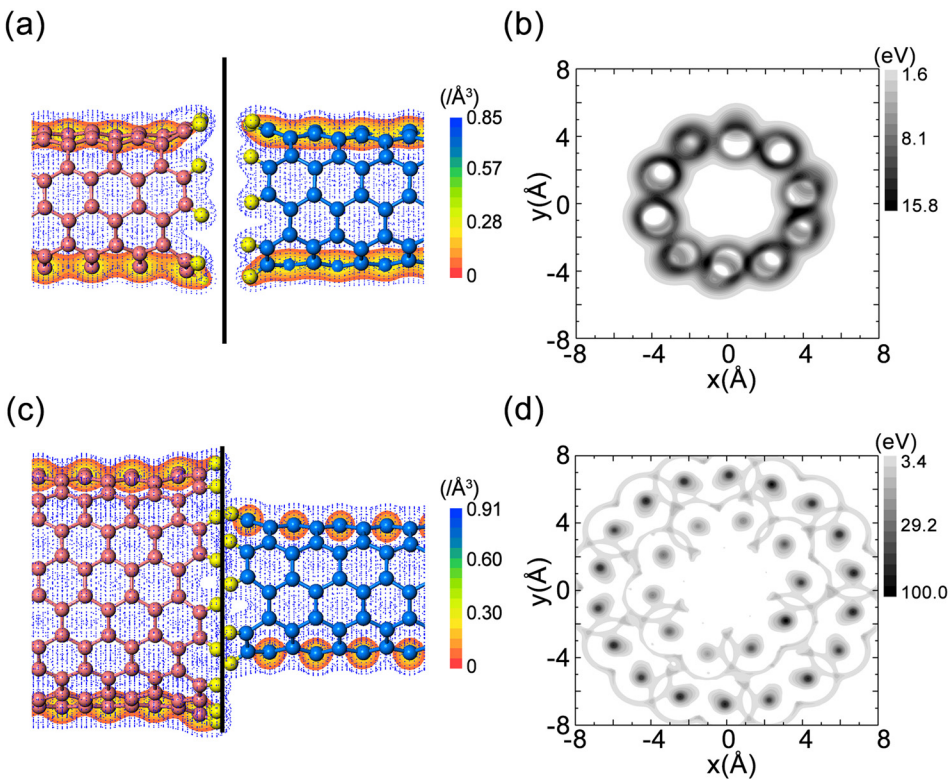

FIG. 5. Electron density distribution near the joint, and the potential distribution on the central section between the adjacent ends of motor and rotor in the armchair models at the 2360^{th} ps: (a) and (b) for the (5, 5) motor with 250 GHz rotational frequency, and (c) and (d) for the (9, 9) motor with 250 GHz rotational frequency. The potential value in (b) and (d) is that of a carbon atom on the plane. Black lines in (a) and (c) represents the interface between the two ends.

on rotor and vice versa. Thus, the distance could change during rotational transmission. As a result, the fluctuation jumps in the rotational frequency of rotor are mainly due to the radial and axial deviations of the rotor's left end from its initial position (Figures 4(a) and 4(b), and Figures 4(c) and 4(d), respectively). The largest deviation is 0.282 nm (>0.265 nm) as shown in Figure 4(d). Hence, the distance gap between the two ends varies from time to time, which leads to the fluctuation of rotational frequency of rotor. This phenomenon also appears in other cases when the (5, 5) motor has a rotational frequency among 200–300 GHz. When driven by the (9, 9) motor with the rotational frequency of 250 GHz, however, there is no obvious fluctuation in the rotational transmission after the stable rotation of rotor is reached. The difference in the rotor's rotational behavior of the two models is due to the different interactions between the adjacent ends of motor and rotor.

Figure 5 shows the electron density distribution (EDD) near the joint and the potential plane in the middle of the joint. It indicates that the interaction between the adjacent ends of motor and rotor is mainly caused by the long range L-J potential rather than the EDD overlap on the adjacent ends. Since the C–H bonds reduce the potential energy on the ends as compared with the model having pure sp^1 bonded carbon atoms on the ends, we can find that the distance gap between two adjacent ends in the (5, 5) model (Figure 5(a)) is higher than that in the (9, 9) model. Therefore, the stronger interaction between carbon atoms on the adjacent ends (Figure 5(d)) leads to the higher rotational frequency of rotor (Figure 2). At the same time, the greater interaction also leads to a more stable configuration of the adjacent ends.

Figure 6 illustrates the time histories of the rotational frequency of rotor in the bearing with (9, 0)/(18, 0) DWCNT when driven by either a (9, 0) or (16, 0) SWCNT-based motor. Each carbon atom on the adjacent ends of the motor and rotor is bonded with a hydrogen atom. The initial gap between the motor and rotor is 0.24 nm. In the zigzag model with the (9, 0) motor (Figure 6(a)), the rotor is actuated easily by the motor. Except for the case by the motor with the rotational frequency of 250 GHz, the rotor rotates synchronously with the motor. Note that the average rotational frequency of the rotor is 177.7 GHz after 1500 ps if it is driven by the motor with the 250 GHz rotational frequency. Therefore, it appears that there is a maximal value in the rotational frequency of rotor driven by the motor with different frequencies. When driven by the (16, 0) motor with the rotational frequency over 200 GHz, the rotor could rotate in a stable way after a quite long duration (Figure 6(b)), e.g., 2700 ps and 5000 ps, respectively. The duration is about 3 or more times of that in the armchair models. It is mainly due to two reasons, i.e., the weaker attraction between motor and rotor, and the higher circumferential potential barrier[24] which hinders the rotor to reach an equilibrium position when interacted with the motor. However, the rotational transmission performs stable as the rotor approaches the equilibrium position.

The behaviors of a rotational transmission system consisting of a SWCNT based-motor and DWCNTs-based bearing are investigated with MD simulation. In the system, the interaction between the two adjacent ends of motor and rotor drives the rotation of rotor, i.e., the inner tube in bearing. As

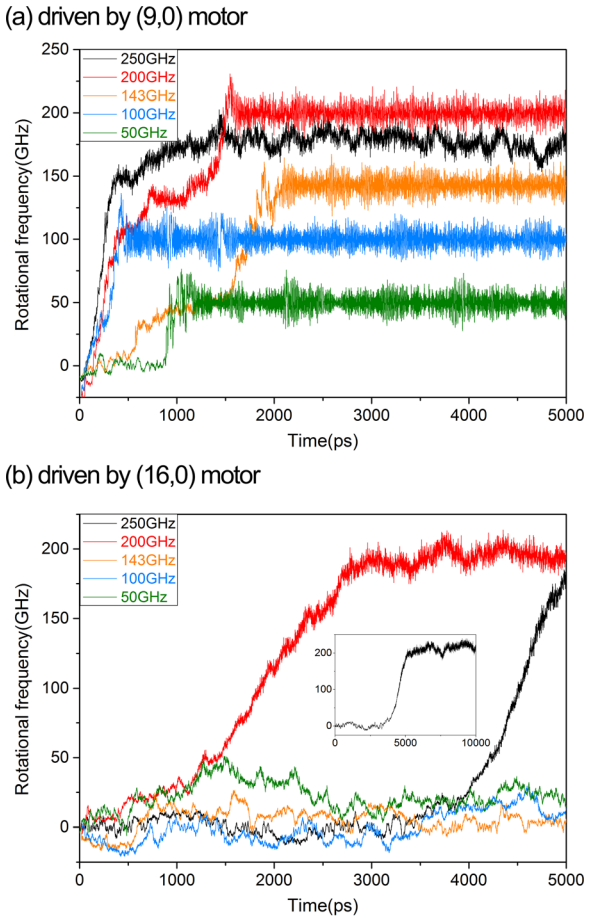

FIG. 6. For the zigzag models, the time histories of the rotational frequency of rotor are shown with different values of rotational frequency of the driving motor (black curve: 250 GHz/4 ps, red curve: 200 GHz/5 ps, orange curve: 143 GHz/7 ps, blue curve: 100 GHz/10 ps, and green curve: 50 GHz/20 ps).

the carbon atoms on the adjacent ends are bonded with hydrogen atoms, the L-J interaction plays a major role in actuating the rotation of rotor. Two conclusions can be drawn as below.

(1) The weak attraction between the motor and rotor leads to the oscillation of the rotor in the outer tube. Meanwhile, the high radial and/or axial deviation of the rotors end leads to the fluctuation in the rotor's rotational frequency during transmission. Hence, a stable rotational transmission system should have a stable configuration of the joint between motor and rotor.
(2) Driven by the motor, the rotor in a zigzag bearing could reach a stable rotation much faster than that in an armchair bearing. For a rotational transmission system with either an armchair or zigzag bearing, a desired stable high-speed (>50 GHz) asynchronous rotational transmission could be obtained if the rotational frequency of motor is very high, e.g., >200 GHz.

This work was supported in part by the National Natural-Science-Foundation of China (Grant Nos. 50908190 and 11232003), the 111 Project (No. B08014), and the Research Foundation (Grant No. GZ1205) of the State Key Laboratory of Structural Analysis for Industrial Equipment, Dalian University of Technology, China.

[1]J. Cumings and A. Zettl, Science **289**(5479), 602 (2000).
[2]Q. Zheng and Q. Jiang, Phys. Rev. Lett. **88**(4), 045503 (2002).
[3]K. Cai, H. Yin, Q. Qin, and Y. Li, Nano Lett. **14**(5), 2558 (2014).
[4]S. Zhang, W. K. Liu, and R. S. Ruoff, Nano Lett. **4**(2), 293 (2004).
[5]B. E. Zhu, Z. Y. Pan, Y. X. Wang, and Y. Xiao, Nanotechnology **19**(49), 495708 (2008).
[6]S. Joseph and N. Aluru, Phys. Rev. Lett. **101**(6), 064502 (2008).
[7]A. Lohrasebi and Y. Jamali, J. Mol. Graphics Modell. **29**(8), 1025 (2011).
[8]R. E. Tuzun, D. W. Noid, and B. G. Sumpter, Nanotechnology **6**(2), 52 (1995).
[9]A. Barreiro, R. Rurali, E. R. Hernandez, J. Moser, T. Pichler, L. Forro, and A. Bachtold, Science **320**(5877), 775 (2008).
[10]H. Somada, K. Hirahara, S. Akita, and Y. Nakayama, Nano Lett. **9**(1), 62 (2009).
[11]I. Santamaría-Holek, D. Reguera, and J. M. Rubi, J. Phys. Chem. C **117**(6), 3109 (2013).
[12]M. F. Yu, B. I. Yakobson, and R. S. Ruoff, J. Phys. Chem. B **104**(37), 8764 (2000).
[13]A. Fennimore, T. Yuzvinsky, W.-Q. Han, M. Fuhrer, J. Cumings, and A. Zettl, Nature **424**(6947), 408 (2003).
[14]B. Bourlon, D. C. Glattli, C. Miko, L. Forró, and A. Bachtold, Nano Lett. **4**(4), 709 (2004).
[15]J. Vacek and J. Michl, Adv. Funct. Mater. **17**(5), 730 (2007).
[16]Z. Tu and X. Hu, Phys. Rev. B **72**(3), 033404 (2005).
[17]B. Wang, L. Vuković, and P. Král, Phys. Rev. Lett. **101**(18), 186808 (2008).
[18]J. W. Kang and H. J. Hwang, Nanotechnology **15**(11), 1633 (2004).
[19]A. Prokop, J. Vacek, and J. Michl, ACS Nano **6**(3), 1901 (2012).
[20]Z. Xu, Q. Zheng, and G. Chen, Phys. Rev. B **75**(19), 195445 (2007).
[21]K. Cai, Y. Li, Q. H. Qin, and H. Yin, Nanotechnology **25**(50), 505701 (2014).
[22]L. T. Scott, E. A. Jackson, Q. Zhang, B. D. Steinberg, M. Bancu, and B. Li, J. Am. Chem. Soc. **134**(1), 107 (2012).
[23]S. J. Stuart, A. B. Tutein, and J. A. Harrison, J. Chem. Phys. **112**(14), 6472 (2000).
[24]Q. W. Hou, B. Y. Cao, and Z. Y. Guo, Nanotechnology **20**(49), 495503 (2009).
[25]Z. Guo, T. Chang, X. Guo, and H. Gao, Phys. Rev. Lett. **107**(10), 105502 (2011).